Title: ATBD cloud albedo and cloud optical thickness

Doc. no: MAPP-ATBD-CACO

Issue: 1

Revision: 1

Date: 05 February 1999

internal Distribution

Name	Quantity

external Distribution

Name	Quantity

Change Record

Issue	Revision	Date	Description	Change pages

Table of Contents

1. INTRODUCTION

1.1 Algorithm Identification

cloud albedo cloud optical thickness

2. ALGORITHM OVERVIEW

The cloud optical thickness and the cloud albedo are major quantities describing the shortwave optical properties of clouds and their influence on the global radiation and energy budget. Measurements from space can be used to map these properties on a global scale. Since the first launch of the TIROS-1 satellite in 1960, remotely sensed data has been used for cloud climatological studies and a series of cloud parameter have been observed. Generally, the characteristics of the platforms and the instrument determine the performance of the retrieval and the way, how the products can be used for further analysis. Starting with the determination of the cloud cover fraction, more sophisticated retrieval techniques could be applied, as the sensors provided more information in terms of the number of channels and spatial resolution as the most important factors. Up to now, most retrieval procedures rely on broadband measurements, while new type of spaceborne imaging radiometers allow narrow-band measurements which eliminate errors due to gaseous absorption.

Due to the large variability in time and space of clouds and water vapour and the non-linear relation between these two factors, it is not possible to produce cloud and water vapour statistics from broadband measurements of the radiative flux.

The MERIS instrument will be a representative of a new generation of satellite sensors in space. A large number of spectral bands with specialized purposes are available together with a moderate spatial resolution. With this combination MERIS can greatly contribute to a better representation of climate relevant processes in global circulation and climate models by providing global and regional data sets to validate the simplified physics represented in these models against observation.

Two channels at 753.75nm and 761nm (channel No. 10 and 11) are especially dedicated to the cloud retrieval, enabling the estimation of the cloud top pressure by and differential absorption approach. The window channel at λ=753.75nm (bandwidth $\Delta\lambda$=7.5nm) is used for ESA's operational MERIS cloud products cloud albedo and cloud optical thickness (Fischer *et al.* ,1998).

The cloud optical thickness and cloud albedo algorithm for the MAPP Project are based on ESA's operational products. In this document we describe the extensions to this products. This mainly refers to an improvement of the operational algorithms in terms of accuracy and quality control as it is made possible due to the restriction to a region of interest and additional information. Additionally, we will provide "value-added products", i.e. parameters derivable from the operational or MAPP specific product in combination with statistics and/or spatial analyses. The products related to cloud albedo and cloud optical thickness to be derived within the MAPP project are:

- cloud optical thickness
- cloud albedo
- cloud optical thickness error
- cloud albedo error
- cloud forcing

3. ALGORITHM DESCRIPTION

3.1 Theoretical Description

3.1.1 Physics of the Problem

The physical basis of the cloud albedo and cloud optical thickness retrieval problem is already described in the ATBD "cloud albedo and cloud optical thickness" (Fischer *et al.*, 1998), which we refer to. In this section, we highlight the approaches for the specific MAPP improvements and additions of the product.

3.1.1.1 cloud albedo and cloud optical thickness

While the procedure of the retrieval of these products remains unchanged for the MAPP analysises, the coefficients used to invert the measured radiance to cloud parameter will be recalculated. The coefficients of the operational products are necessarily fixed and they are calculated to be valid for most of the MERIS measurements. The restriction to one specified region (European continent) enables a more precise and specified calculation of the regression coefficients. It is believed, that therefore the MERIS cloud products for this region can be improved within the MAPP algorithms.

3.1.1.1.1 parameter selection

The problem of all applications based on inversion techniques is that the validity is restricted to the range of input data as used for the inversion process and is dependent on the quality of the input data. We therefore plan to select carefully the set of input parameters, which we use for the radiative transfer simulations, the basis of the inversion with regression. Existing cloud statistics and climatologies, such as the International Satellite Cloud Climatological Project ISCCP (Schiffer and Rossow, 1983) provide the information of the range and the frequency of cloud properties. The MAPP coefficients will be created with the aid of these information. The following input parameters for the radiative transfer calculations will be selected stochastically according to the ISCCP statistics of the MAPP region:

- cloud top height
- cloud type (effective radius)
- cloud optical thickness

3.1.1.1.2 angular resolution

The MAPP region is defined to be completely north of the tropic of cancer, meaning that the MAPP algorithm for the cloud albedo and cloud optical thickness does not need to consider the full range of solar zenith angles, because the minimum value is less than in the case of the operational algorithm. Additionally, the overpass times restrict the range of occurring solar zenith angles for the MAPP region. The algorithm development will benefit from that fact by calculation the regression coefficients for an higher angular resolution, which will not increase the size of the coefficient database.
For the MAPP algorithms, coefficients will be available with an angular resolution of 1° compared to the 2.5° resolution of ESA's operational products. The error due to interpolation of the coefficients to the actual sun zenith , viewing zenith and azimuth angles of the pixel will be reduced.

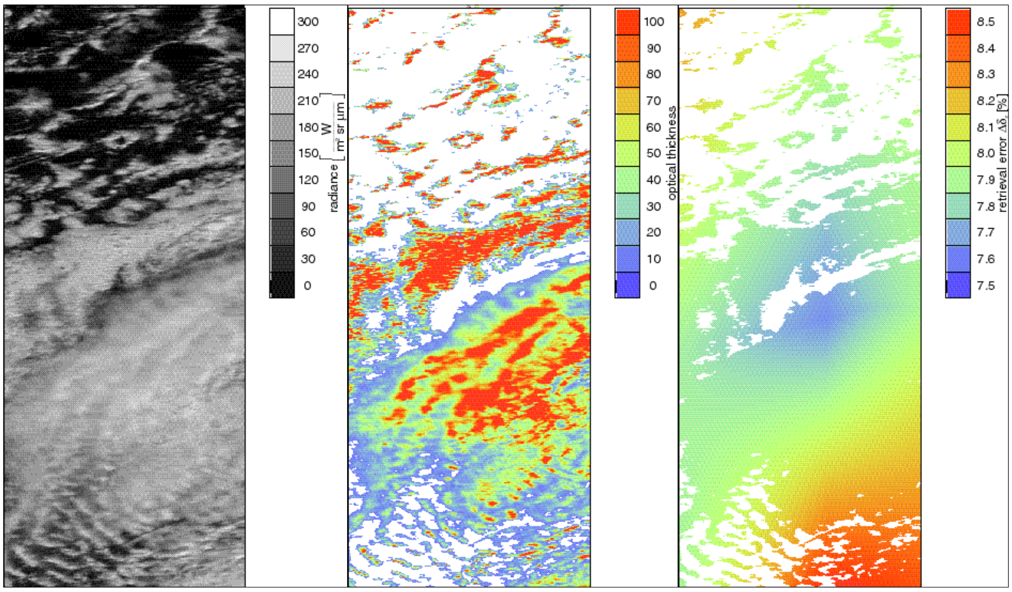

Figure 1: Application of the MAPP optical thickness algorithm to an image recorded by the Modular Optoelectronical Scanner MOS at 3. April 1998 near the cost of Ireland. Radiance measured in the MOS channel at 750nm (left) retrieved optical thickness (middle) and the relative retrieval error (RMSE) in percent (right):

3.1.1.1.3 surface albedo consideration

An estimate for the surface albedo is needed for the cloud optical thickness and cloud albedo retrieval, because of the large influence of ground reflection even under thicker clouds. The operational product is using surface albedo data from the International Satellite Land Surface Climatology Project ISLSCP (Sellers et al. 1996), which is fixed during the operational phase of the MERIS mission. The MAPP products can be designed much more flexible concerning the input information of the surface albedo. Therefore, an dynamic update of the used database is planned for the cloud and water vapour retrieval. Update information will come from previous MERIS overpasses and the MAPP land surface products.

3.1.1.2 Error estimate CA / COT

Some improvements of the cloud albedo / cloud optical thickness algorithm itself are described in the previous sections of this document. They will reduce errors and uncertaincy compared to the operational product, but still, large inaccuracies will remain due to physical limitations of the retrieval, e.g. at high solar zenith angles and large optical thickness the retrieval of the optical thickness becomes more difficult.
Therefore, it is important to provide the end user with a measure of quality to display the reliability of the data. This kind of information can avoid misinterpretation and enables the user to decide, which part of the images or data he needs to exclude in his analysis.
An other important use of the error information is the calculation of Level 3 products, e. g. monthly averages of the Level 2 products. In the Level 3 algorithms, each pixel will be checked to be in the range of acceptable accuracy before being included in the averaging process.
The error product is the root mean square error (RMSE) as calculated simultaneously to the coefficients. This will be an relative error and will be produced for each pixel. An example of an error image is shown in Figure 1 (right).

3.1.1.3 Cloud forcing

Cloud forcing is defined as the difference between the upward-directed radiative flux at the top of a cloudy atmosphere and its value, if the clouds would be absent. This is a useful parameter to describe the influences of clouds on the radiative and energy budget, especially for studies on cloud - climate feedback effects. Practically, it is not possible to measure the cloud forcing directly by remote sensing or in situ techniques, because it would require two identical atmopsheric columns: a cloud free and a cloudy one. One approach for a cloud forcing estimation from satellite imaginary is to take radiance measurements of cloudy pixels, convert them to fluxes by assuming isotropic reflection and to relate them to cloud free fluxes gathered from pixels nearby, assuming that there are no variation of other atmospheric quantities between the two pixels. It is quite obvious, that the accuracy and validity of this approach increases with the spatial resolution of the satellite sensor. In contrast, our approach of an MAPP product cloud forcing will pixel-based and a straight forward calculation. For each cloudy pixel the upward directed flux at top of atmosphere can be calculated from cloud albedo and the solar irradiance at 753.75nm. This value will be related to an upward directed flux, estimated from the surface properties of that pixel and an average atmospheric state as observed in previous MERIS overpasses.
This product will combine cloud-, land surface- and aerosol products developed for the MAPP project.

3.1.2 Mathematical Description of the Algorithm

3.1.2.1 cloud albedo and cloud optical thickness

A mathematical description of the cloud albedo and cloud optical thickness algorithm is given in ATBD of the operational ESA product (Fischer *et al.*, 1998). The structure of the MAPP products is identical to these described in that document.

3.1.2.2 RMSE cloud albedo and cloud optical thickness

The regression calculates the coefficients for each combination of solar and observational angles and surface albedo on the basis of radiances simulated for a number of cases according to realistic statistics. The root mean square error of the optical thickness regression is defined as the sum of the squared deviation between the true optical thickness d_c and the optical thickness d_c' calculated with the polynomial expression using the coefficients divided with the number N of simulated cases used for the regression:

$$RMSE = \frac{\sqrt{\sum_{n=1}^{N} \left(d_c' - d_c\right)^2}}{N}.$$

The RMSE for the cloud albedo is calculated in the same way. These RMSE´s are determined in parallel to the regression process and stored in separate database with the same angular resolution as the regression coefficients. Similar to the coefficient selection, the RMSE´s of a cloudy MERIS pixel can be extracted using the pixel values of the solar zenith angle, viewing zenith angle and the azimuthal difference as well as the surface albedo (Figure 2).

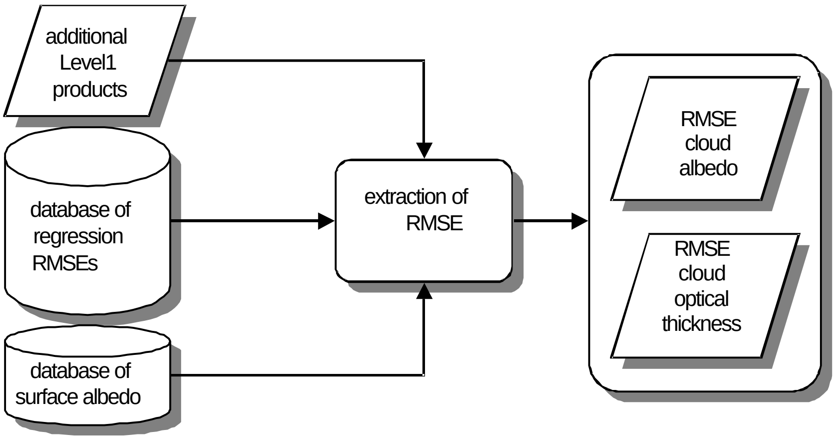

Figure 2: Flowchart diagram of the inversion process of the root mean square errors of the cloud albedo and cloud optical thickness retrieval.

3.1.2.3 cloud forcing

TBD

3.2 Practical Considerations

TBD

3.2.1 Numerical computation considerations

TBD

3.2.2 Calibration and Validation

TBD

3.2.3 Quality Control and Diagnostics

TBD

3.2.4 Exception Handling

TBD

3.2.5 Output Products

- cloud albedo
- cloud optical thickness
- RMSE cloud albedo
- RMSE cloud optical thickness
- cloud forcing

4. ERROR BUDGET ESTIMATES

The influence of the regression on the accuracy of the retrieved product is shown in Figure 3 for cloud optical thickness and for cloud albedo as a function of solar zenith angle and viewing zenith angle. Both graphs show that the retrieval of cloud optical thickness as well as the retrieval of cloud albedo is more difficult for larger solar zenith angles. The Figure shows clearly the higher sensitivity of the cloud optical thickness retrieval on solar zenith angle compared to the cloud albedo retrieval.

This study is focused on a sensitivity analysis which considers the influence of the observation geometry within a representative MERIS swath, the instrumental noise as well as other atmospheric and surface properties on the accuracy of the retrieved cloud product. Since a complete sensitivity study would require a systematic and

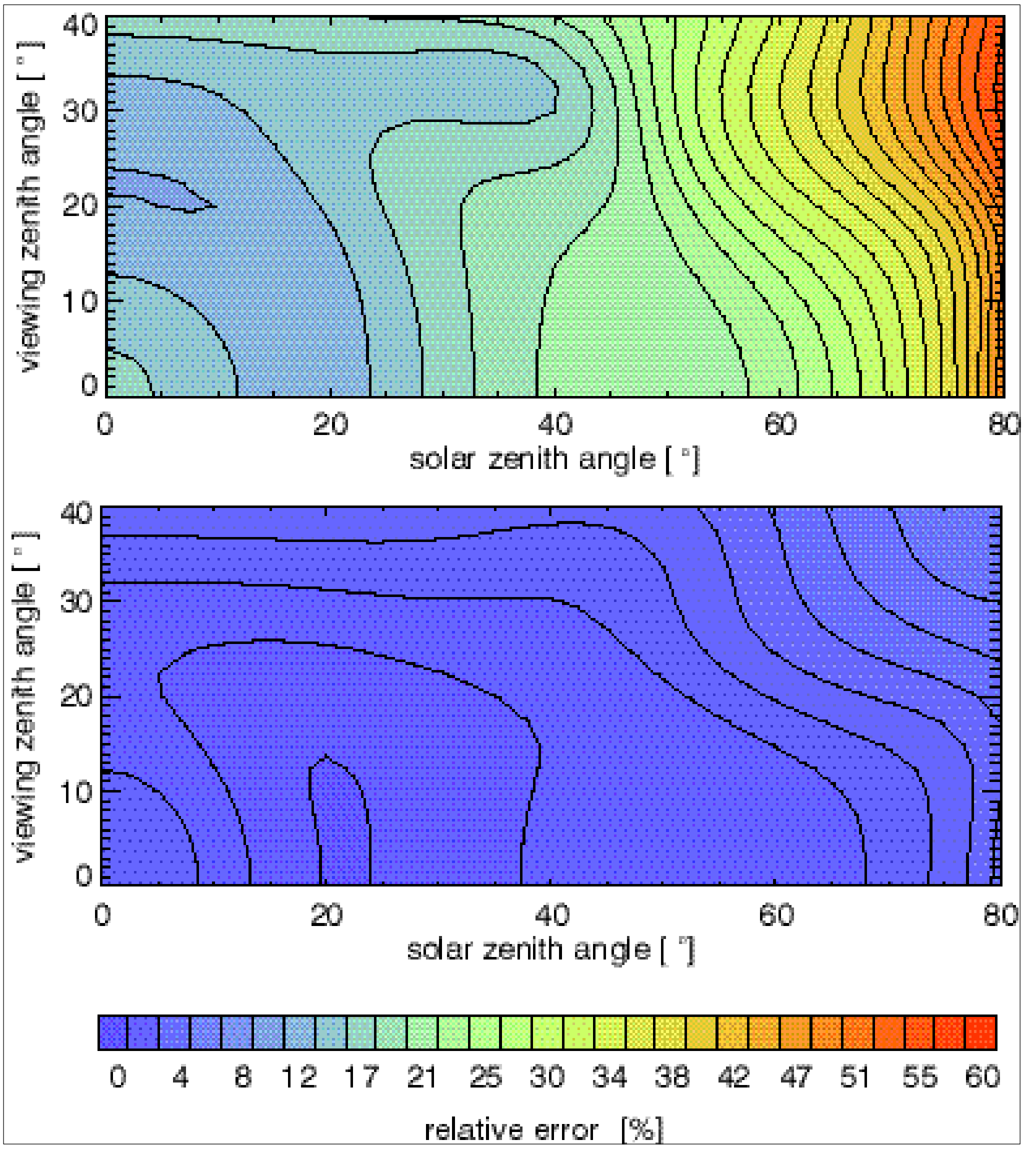

Figure 3: Relative error in percent in retrieved cloud optical thickness (upper graph) and cloud albedo (lower graph) due to regression errors as a function of viewing zenith angle J_v and solar zenith angle J_s (azimuthal difference $Df = 90°$, surface Albedo $a_s = 0\%$).

independent variation of all these parameters which is quite difficult to achieve, we reduced the number of combinations by limiting the range of parameters to values as they occur during a representative MERIS swath.

Two steps are performed to access the quality of the algorithm. Firstly, the radiance values for each pixel of the swath have been computed as a function of the parameter under investigation, by using radiative transfer simulations of MERIS Channel 10 and 11. In a second step, we applied the MERIS cloud albedo, cloud optical thickness and cloud top pressure algorithms to these pseudo MERIS images. Beside the images, swath averages of retrieved values, deviations and relative errors are produced in order to quantify the overall effect of the influencing parameters. Projections of the swath images to a map should help to identify geographic regions, where the retrieval is critical (e. g. high solar zenith angles at high latitudes).

4.1.1 Simulation of MERIS images

The properties of the considered MERIS swath simulation are listed in Table 1. This particular swath has been selected, because it covers areas over ocean (70% of all pixels) and land surfaces of different reflectivity (30 % of all pixels) which is quite representative for the land-ocean coverage fraction of the whole earth. The orbital parameter of ENVISAT and the viewing geometry of the MERIS sensor has been used to calculate longitude and latitude as well as the solar and viewing zenith angle and the azimuth difference of each pixel.

The land surface albedo is taken from the data-set of the *International Satellite Land Surface Climatology Project* ISLSCP (Sellers *et al*. 1995). The surface albedo is an integrated value over the entire solar spectrum, thus no wavelength dependencies are considered. Because of the very large solar zenith angles in the northern and southern part of the swath where an estimate of cloud top pressure, cloud optical thickness and cloud albedo is not possible, we restricted our analysis to the range between 70° N and 55° S latitude.

Table 1: Properties of the considered MERIS swath.

Day of the year	80
Measuring time	1100 sec
Satellite inclination	1.72°
Satellite altitude	799 km
Equator crossing time	10:00
Latitude range	70°N – 55°S
Longitude range	15°E – 29°W
Solar zenith angle range	26° - 71°
Viewing zenith angle range	0° - 40°
Azimuth difference range	0° - 180°
Surface albedo range	0% - 40%

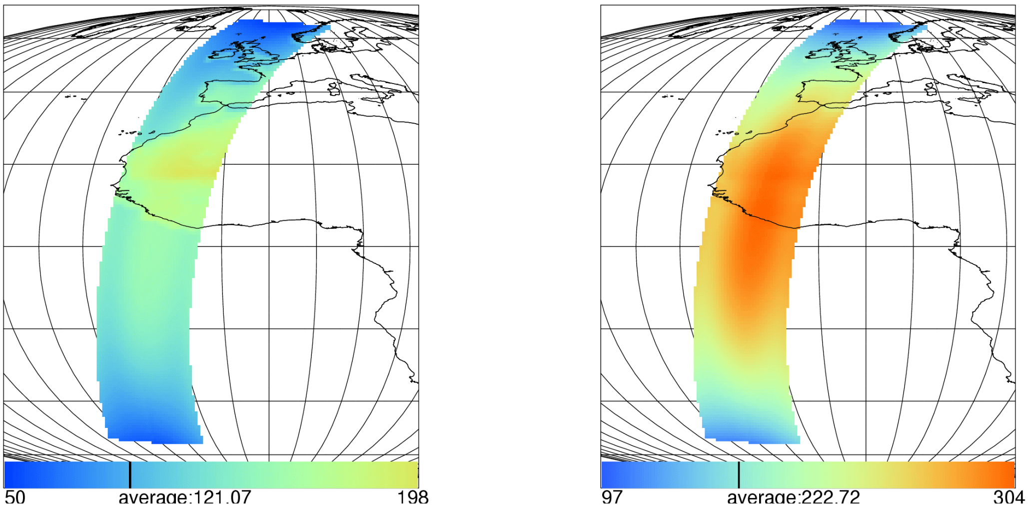

Figure 4: Simulated MERIS swath with radiances at channel 10 (753.75nm) calculated with a cloud optical thickness of δ_c = 10 (left) and δ_c = 50 (right).

4.1.2 Cloud optical thickness

4.1.2.1 Sensitivity to geometry

Retrieved cloud optical thickness along a MERIS swath is shown in Figure5. The optical thickness, assumed for the radiative transfer simulations, is constant for the entire swath. Even for δ_c = 10 (left) the surface structure nearly disappears. The algorithm seems to under-estimates the optical thickness for observation geometries which are closer to the edge of the swath.
At higher latitudes the optical thickness is overestimated. For this MERIS swath averages of δ_c(swath-average) = 8.05 (left) and δ_c(swath-average) = 47.54 (right) have been retrieved.

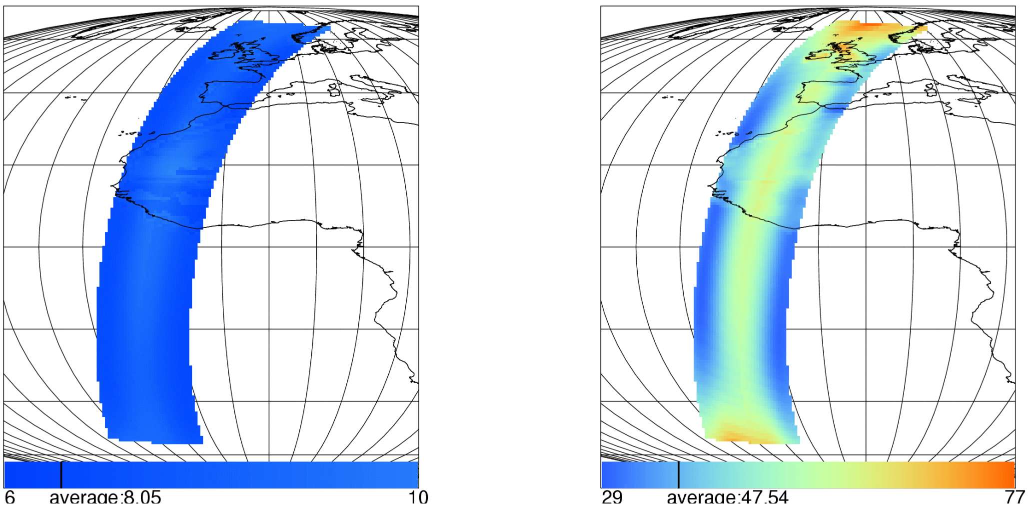

Figure 5: Retrieved cloud optical thickness from simulated MERIS measurements calculated with a cloud optical thickness of δ_c = 10 (left) and δ_c = 50 (right).

4.1.2.2 Sensitivity to cloud optical thickness and cloud top height

The sensitivity to cloud optical thickness and cloud top height variations has been analysed with the general finding, that the RMSE (root mean square error) increases with optical thickness. For typical values of $\delta_c = 50$ a RMSE = 9 has been estimated. The influence of the cloud top height is obvious with a general tendency to higher RMSE values for higher cloud top heights. The root mean square error RMSE (upper graph) and BIAS (lower graph) is shown in Figure 6. The BIAS drastically increases with cloud top heights. Optically thick and low clouds are underestimated with respect to the optical thickness

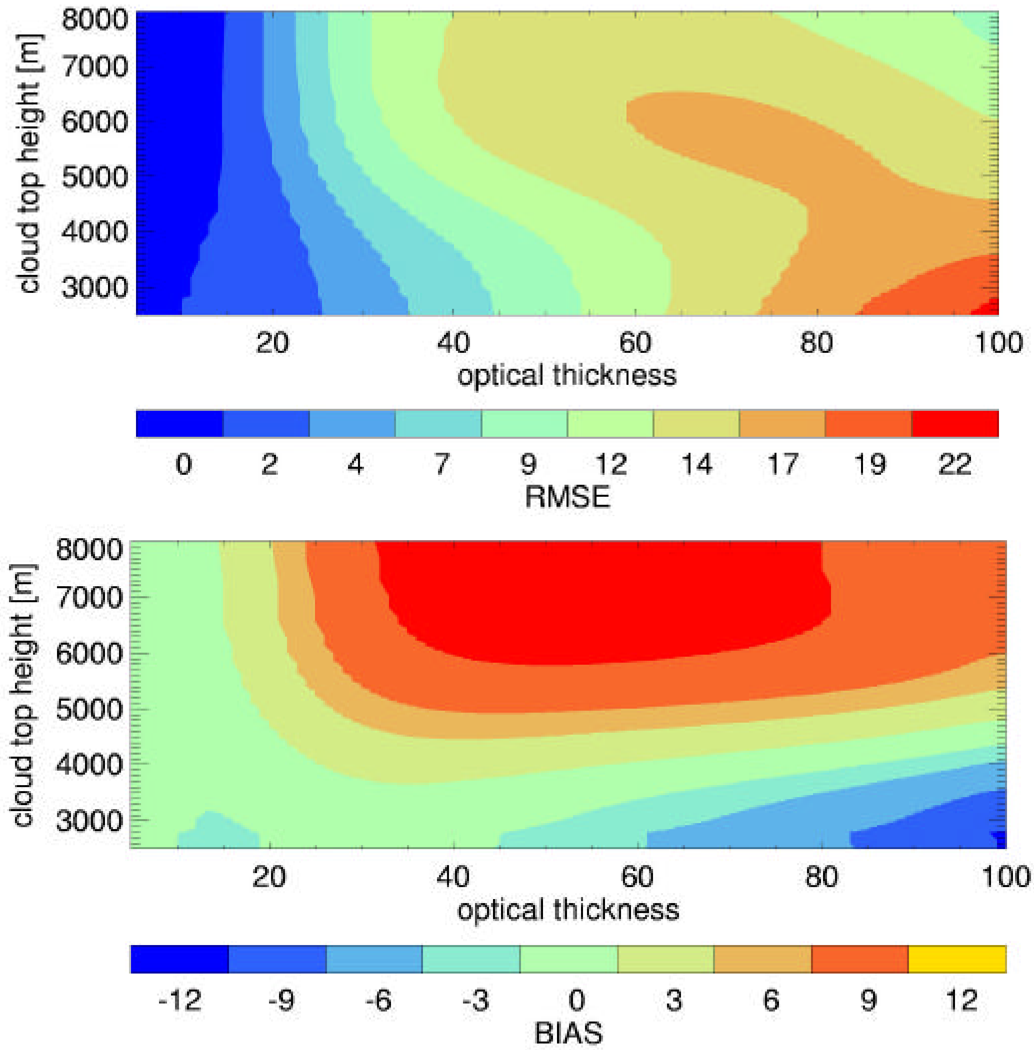

Figure 6: Sensitivity of the cloud optical thickness retrieval to cloud optical thickness and cloud top height. Root mean square error RMSE (upper graph) and BIAS (lower graph).

4.1.2.3 Sensitivity of cloud optical thickness retrieval to surface albedo

The sensitivity of the cloud optical thickness retrieval to the surface albedo is shown in Figure 7. The root mean square error RMSE (upper graph) is lower at high and low surface albedo values when the optical thickness is smaller than 50. The largest errors occurs at surface albedos of 50% and high optical thickness. These results have to be interpreted with respect to the algorithm development which is driven by the minimisation of the overall errors.

The lower graph of Figure 4 is showing the BIAS of the retrieved optical thickness. The lowest values for the BIAS are found for optical thicknesses of $\delta_c \sim 50$.

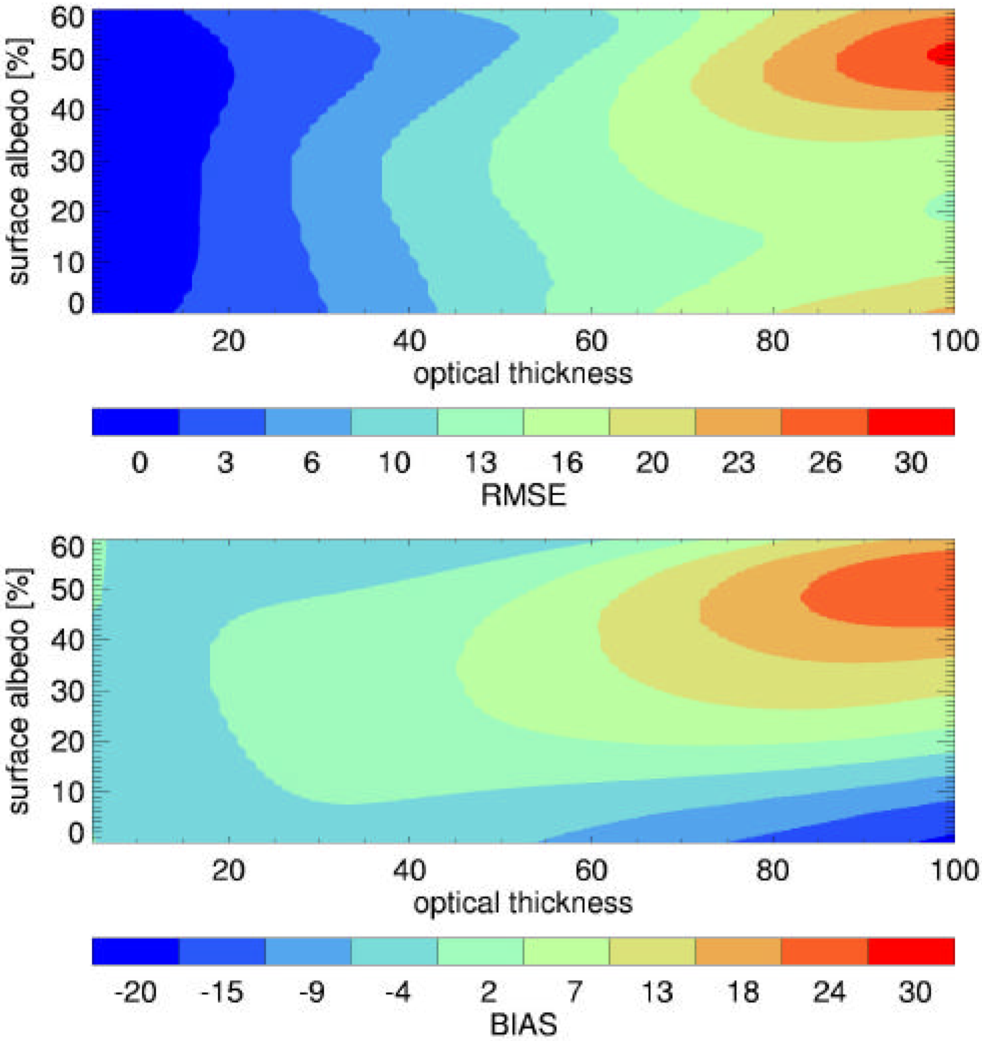

Figure 7: Sensitivity of the cloud optical thickness retrieval to cloud optical thickness surface albedo. Root mean square error RMSE (upper graph) and BIAS (lower graph).

4.1.2.4 Sensitivity to cloud optical thickness and instrumental noise

Figure 8 shows the sensitivity of the cloud optical thickness retrieval to cloud optical thickness and instrumental noise. The sensitivity of cloud optical thickness to instrumental noise is low compared to the sensitivity to other parameters. Within the considered range RMSE values between 0.03 and 0.07 % are found. The BIAS is more important and reaches values up to δ_c ~ -12.

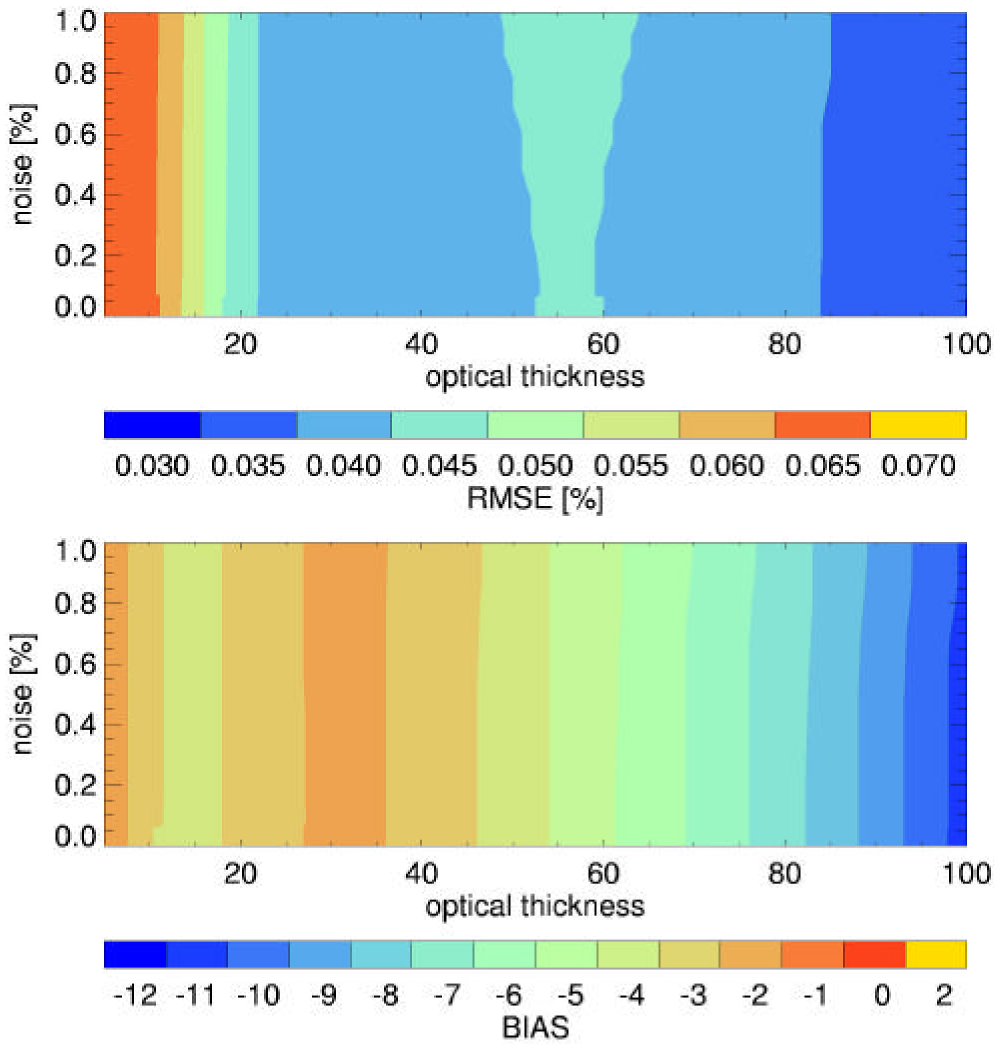

Figure 8: Sensitivity of the cloud optical thickness retrieval to cloud optical thickness and instrumental noise. Root mean square error RMSE (upper graph) and BIAS (lower graph).

4.1.3 Cloud albedo

4.1.3.1 Sensitivity to cloud optical thickness and cloud top height

The sensitivity of the cloud albedo retrieval to cloud optical thickness and cloud top height is shown in Figure 9. For higher optical thickness and cloud top height the RMSE of the albedo retrieval decreases. In most of the cases the RMSE is below 0.04 %. The BIAS is in the same range.

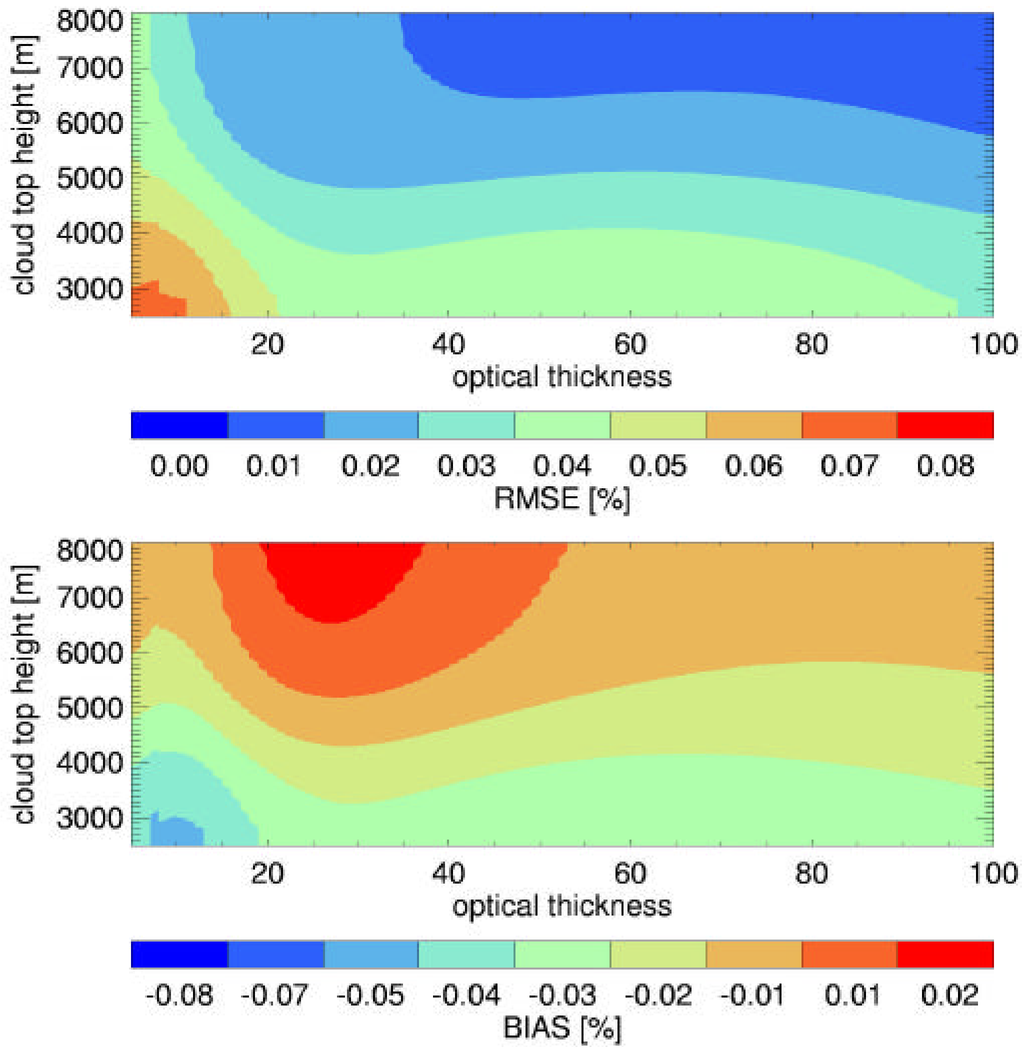

Figure 9: Sensitivity of the cloud albedo retrieval to cloud optical thickness and cloud top height. Root mean square error RMSE (upper graph) and BIAS (lower graph).

4.1.3.2 Sensitivity to cloud optical thickness and surface albedo

The sensitivity of the cloud albedo retrieval to cloud optical thickness and surface albedo is shown in Figure 10. The root mean square error (upper graph) is lowest for high cloud optical thickness and mean surface albedo values between 20 and 60 %. For most of the measuring conditions the RMSE is below 0.03 %. The BIAS (lower graph) is between –0.01 and 0.01 %.

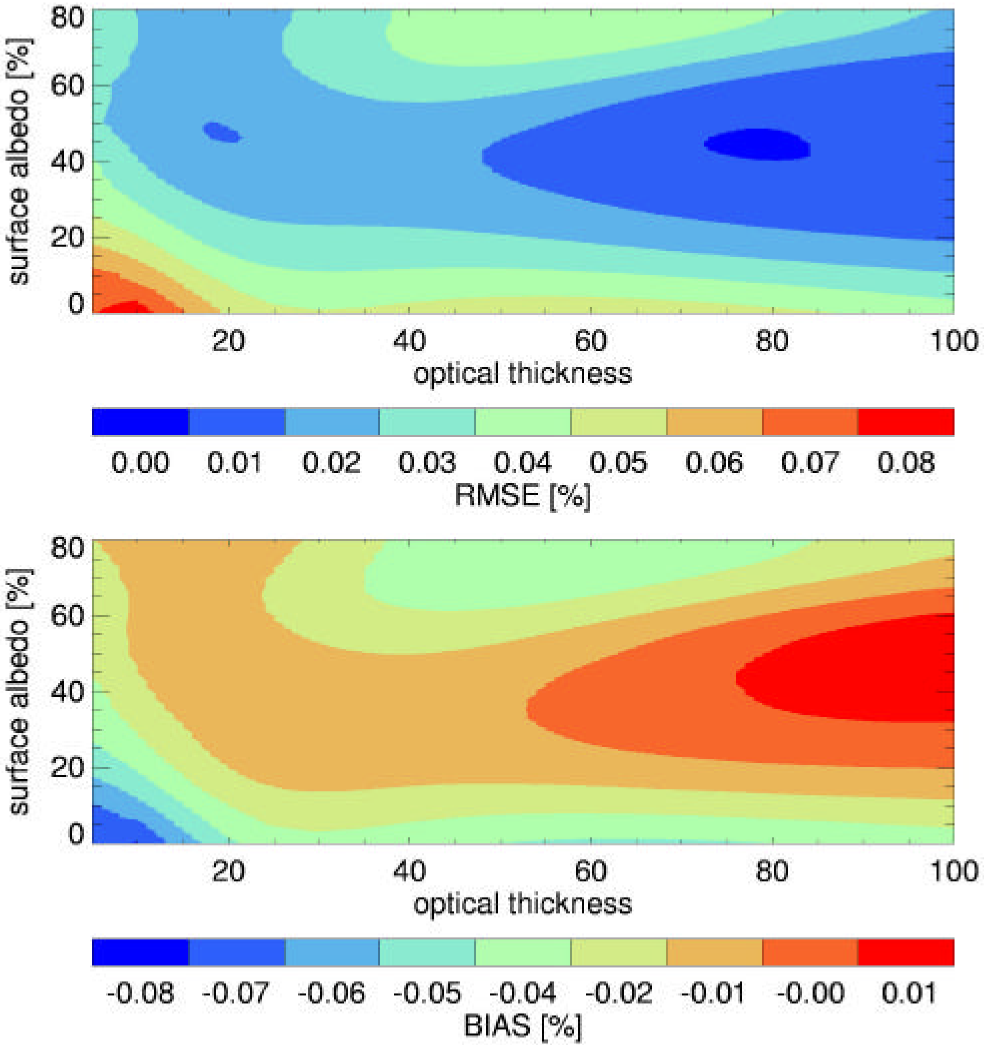

Figure 10: Sensitivity of the cloud albedo retrieval to cloud optical thickness and surface albedo. Root mean square error RMSE (upper graph) and BIAS (lower graph).

4.1.3.3 Sensitivity to cloud optical thickness and instrumental noise

The sensitivity of the cloud albedo retrieval to cloud optical thickness and instrumental noise is shown in Figure 11. The root mean square error is in most of the considered cases is below 0.04 % (upper graph). The negative BIAS is below 0.03% (lower graph).

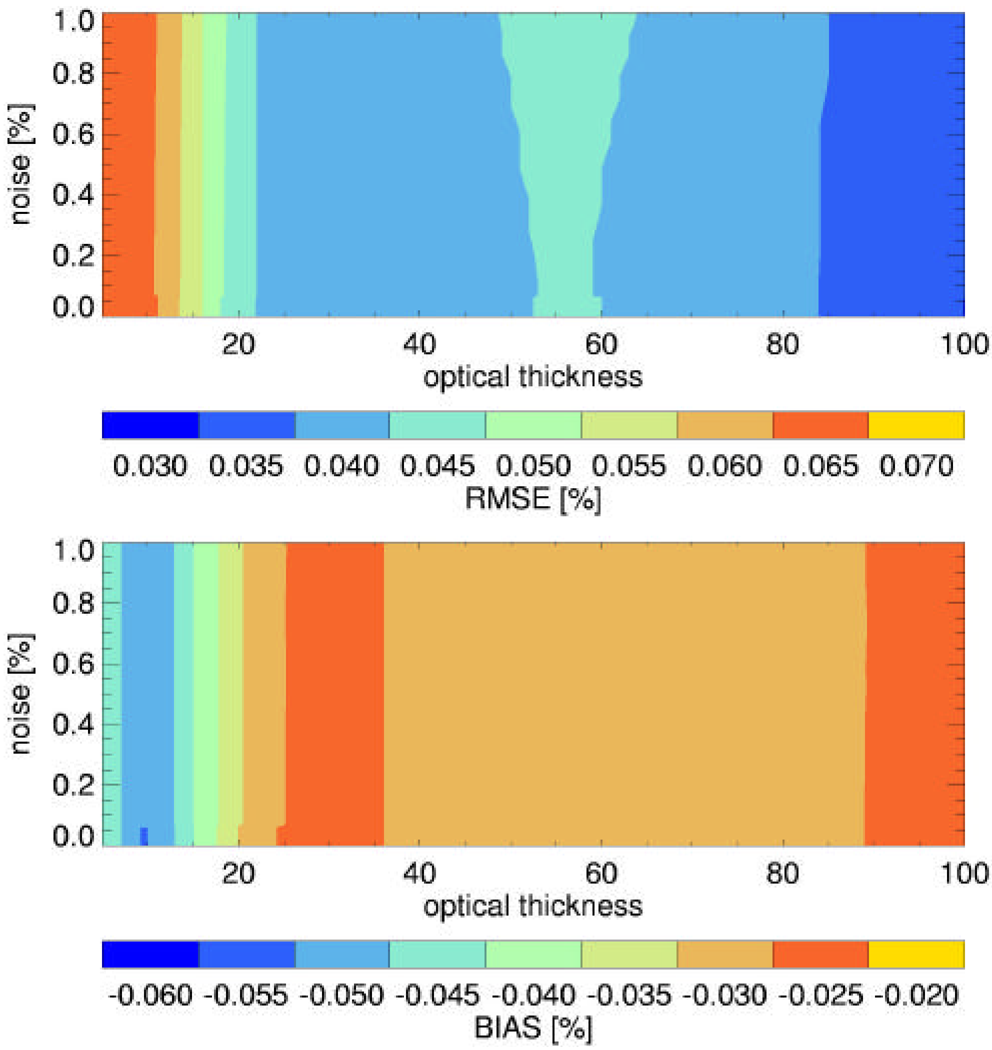

Figure 11: Sensitivity of the cloud albedo retrieval to cloud optical thickness and instrumental noise. Root mean square error RMSE (upper graph) and BIAS (lower graph).

5. ASUMPTIONS AND LIMITATIONS

TBD

6. REFERENCES

Fischer, J., L. Schüller, and R. Preusker, 1998: Cloud albedo and cloud optical thickness. Algorithm technical basis document 2.2. ESA Doc. No.: PO-TN-MEL-GS-0005.

Sellers, P.J., W. Meeson, J. Closs, J. Collatz, F. Corprew, D. Dazlich, F. G. Hall, Y. Kerr, R. Koster, S. Los, K. Mitchell, J. McManus, D. Meyers, K.-J. Sun, and P. Try, 1996: The ISLSCP Initiative I global datasets: Surface boundary conditions and atmospheric forcings for land-atmosphere studies. *Bull. Amer. Meteor. Soc.*, **77**, 1987-2005.

Schiffer, R.A., and W.B. Rossow, 1983: The International Satellite Cloud Climatology Project (ISCCP): The First Project of the World Climate Research Programme, *Bull. Amer. Meteor. Soc.*, **64**:779-784.

MAPP data product summary sheet

Product name:	cloud albedo	cloud optical thickness	cloud albedo error	cloud optical thickness error	cloud forcing
Product code:					
Product Level:	2	2	2	2	2
Description of the Product:					
Product Parameters:					
Coverage					
Packaging:					
Units:	1	1	1	1	W/m^{-2}
Range:	0-1	0-300	0-1	0-300	-
Sampling:					
Resolution:					
Accuracy:					
Geo-location:					
Format:					
Appended data:					
Frequency of generation:					
Size of product:					
Additional information:					
Identification of bands used in algorithm	channel 10	channel 10	channel 10	channel 10	channel 10
Assumption on MERIS input data					
Identification of ancillary and auxiliary data					
Assumptions on ancillary and auxiliary data					